World Journal of Advanced Engineering Technology and Sciences

eISSN: 2582-8266

Cross Ref DOI: 10.30574/wjaets

Journal homepage: https://wjaets.com/

(Research Article)

Check for updates

Optimization of solar energy using artificial neural network vs recurrent neural network controller with positive output super lift Luo converter

Kasim Ali Mohammad * and Sarhan M. Musa

Department of Electrical and Computer Engineering, Prairie View A&M University, Prairie View, TX, USA.

World Journal of Advanced Engineering Technology and Sciences, 2024, 12(02), 133–154

Publication history: Received on 31 May 2024; revised on 08 July 2024; accepted on 11 July 2024

Article DOI: https://doi.org/10.30574/wjaets.2024.12.2.0289

Abstract

In today's world, the need for clean energy is crucial. Historically, Renewable energy sources like hydropower, wind, and solar offer sustainable solutions. Photovoltaic (PV) systems convert sunlight into electricity using semiconductor PV cells, which have been efficient for over 30 years. PV cell efficiency depends on irradiance (solar photon intensity) and temperature. Higher irradiance increases efficiency, while higher temperatures decrease it. PV systems, despite low voltage outputs, can be optimized using DC-DC Positive Output Super Lift Luo converters to match load requirements, enhancing system efficiency. Solar irradiance varies throughout the day, affecting PV cell output. Maximum Power Point Trackers (MPPTs) adjust the system's operating point to maintain peak efficiency. This study focuses on designing AI controllers to manage MPPT. We compare the performance of Artificial Neural Networks (ANN) and Recurrent Neural Networks (RNN) using three datasets. The goal is to identify the most efficient AI controller for optimizing solar energy systems.

Keywords: Artificial neural network; DC-DC positive output super lift luo converter; Maximum power point tracking; Photovoltaic system; Recurrent neural network

1. Introduction

In the past, energy generation predominantly involved burning fossil fuels such as coal, oil, and natural gas, converting their chemical energy into heat, and subsequently using this heat to generate electricity through various methods. Unfortunately, this reliance on fossil fuels has significantly contributed to harmful greenhouse gas emissions over the last 70 years, primarily carbon dioxide, exacerbating global climate change. To mitigate these environmental impacts, there is a growing shift towards cleaner and more efficient energy conversion methods, notably photovoltaic (PV) systems [1-2].

PV systems directly convert sunlight into electricity using PV cells. However, the output voltage from PV cells is typically low, necessitating the use of DC-DC converters to increase voltage levels. In this context, the DC-DC Positive Output Super Lift Luo converter plays a crucial role. This converter not only boosts the voltage output but also matches the impedance between the PV system and its connected load, addressing one of the key challenges in optimizing PV system efficiency [3].

Solar irradiance, which represents the intensity of sunlight photons, varies continuously throughout the day. Concurrently, ambient temperature fluctuates based on environmental conditions, affecting the PV system's performance. To maximize energy capture and efficiency, a Maximum Power Point Tracker (MPPT) is employed. The MPPT adjusts the operating point of the PV system in real-time to ensure it operates at its maximum power point (MPP), where the output power is optimized. This adjustment is critical as it aligns with the varying maximum voltage curve of

* Corresponding author: Kasim Ali Mohammad

the PV cells throughout the day. The MPPT signal guides the DC-DC Positive Output Super Lift Luo converter, which uses components like Insulated Gate Bipolar Transistor (IGBT) diodes to control its duty cycle. By modulating the duty cycle, the converter adjusts the output voltage to match the load requirements effectively [4].

Given the non-linear and dynamic nature of solar irradiance (G) and temperature (T), traditional time domain controllers may not efficiently manage these variations [5]. Therefore, artificial intelligence (AI) controllers offer a more effective solution. In this study, two AI controller methods, Artificial Neural Networks (ANN) and Recurrent Neural Networks (RNN), are considered. These AI controllers excel in handling non-linear changes in input values from PV cells, thereby optimizing control efficiency and enhancing overall system performance [6-7].

The transition from fossil fuel-based energy generation to renewable sources like PV systems represents a significant step towards sustainability. By integrating advanced technologies such as MPPTs, DC-DC converters, and AI controllers, we can effectively harness solar energy while maximizing efficiency and minimizing environmental impact.

This paper is sectioned as:

1.1. Section 2: PV System Description and Modelling

- Detailed description of the modeled 213.15-Watt PV array.
- Explanation of the basic block model of PV arrays.
- Discussion on the construction and operation of solar cells based on p-n semiconductor junctions.
- Inputs (G and T) and outputs (voltage output and power output) of the PV array model.
- Methods used for simulating and characterizing the PV system under different conditions.
- DC – DC Positive Output Super Lift Luo Converter Design and Model.

1.2. Section 3: Methodology of ANN Controller

- Introduction to artificial intelligence (AI) controllers.
- Description of Artificial Neural Network (ANN) model used.
- Explanation of how this AI ANN controller is implemented for optimizing the PV system, particularly focusing on its ability to handle non-linear and dynamic inputs (G and T).

1.3. Section 4: Methodology of RNN Controller

- Introduction to artificial intelligence (AI) controllers.
- Description of Recurrent Neural Network (RNN) model used.
- Explanation of how this AI RNN controller is implemented for optimizing the PV system, particularly focusing on its ability to handle non-linear and dynamic inputs (G and T).

1.4. Section 5: Results and Discussion

- Presentation of the results obtained from the ANN and RNN controllers.
- Comparative analysis of the performance of ANN and RNN in optimizing the PV systems.
- Discussion on the strengths and weaknesses of each AI controller method.
- Interpretation of the results in relation to the efficiency and effectiveness of PV system optimization.

1.5. Section 6: Conclusion

- Summary of the key findings from the study.
- Contributions to the field of renewable energy and PV system optimization.
- Recommendations for future research directions.
- Closing remarks on the potential impact of using AI controllers in enhancing PV system performance.

2. PV System description and modelling

We provide a detailed description of the PV system model, its components, and the integration of ANN and RNN controllers, along with block diagrams illustrating the proposed models [8]. The PV array model has Inputs: Solar Irradiance (G) and Temperature (T) with two outputs for ANN controller: Output Voltage and Output Power, and one output for RNN controller: Output Voltage. A DC-DC Positive Output Super Lift Luo Converter, the Role of MPPT in the PV system is maximizing the power output by adjusting the operating point. The Generation of reference voltage (Vpv) is based on calculations and predictions from ANN or RNN algorithms. The PV system is directly connected to a fixed load. The block diagrams Fig. 1, and Fig. 2, serve to visually clarify the system's architecture and control flow [9-10].

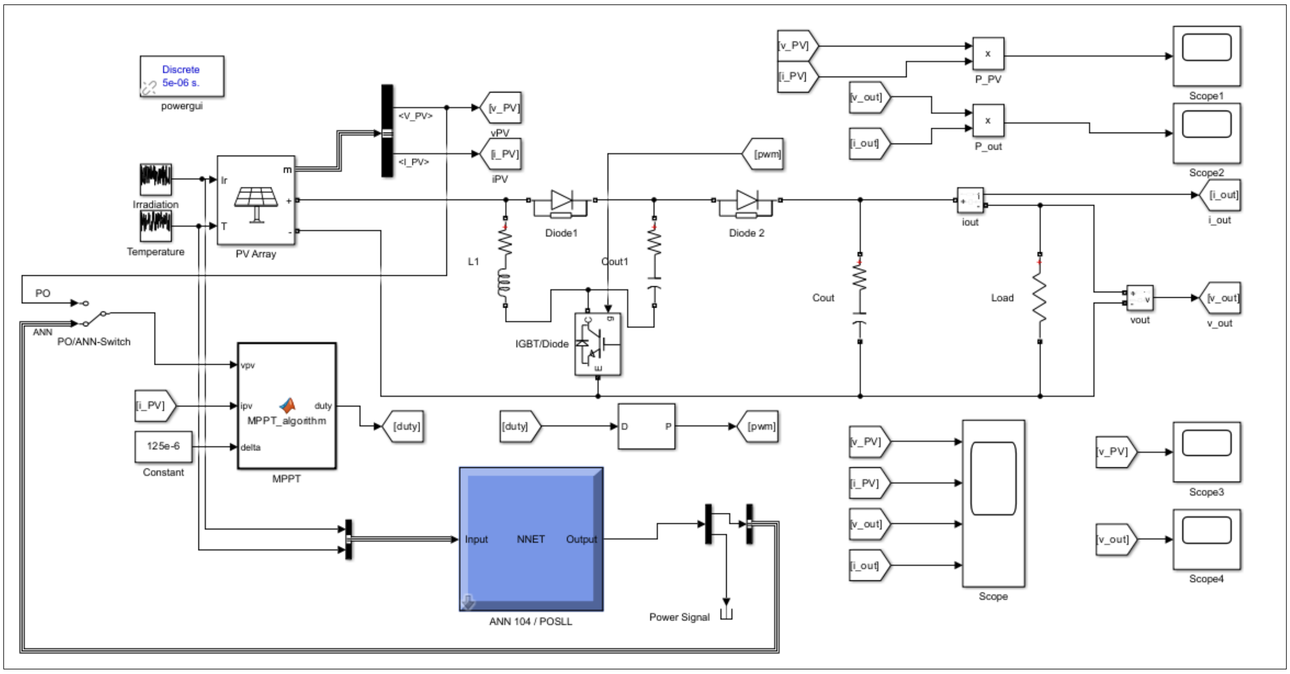

Figure 1 Block diagram for the proposed designed ANN model

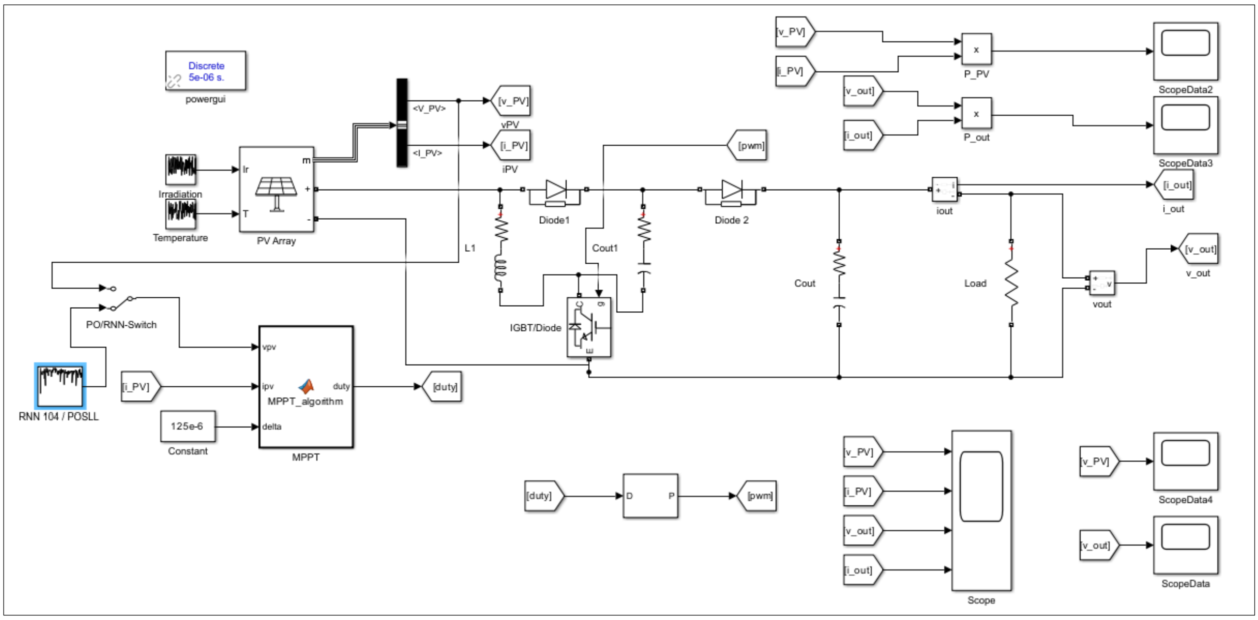

Figure 2 Block diagram for the proposed designed RNN model.

2.1. Mathematical Solar Array Modelling

The single-diode model is widely used for modeling photovoltaic (PV) cells. This model includes the following components:

- Photo-current source (I_{ph}): Represents the current generated by the solar cell when exposed to sunlight.
- Diode (D): Models the p-n junction of the solar cell, providing a path for the recombination of charge carriers.

- Series Resistance (R_s): Represents the resistive losses within the cell.
- Shunt Resistance (R_{sh}): Represents leakage currents within the cell.

The equivalent circuit of a PV cell using the single-diode model can be represented as follows:

$$I = I_{ph} - I_D - I_{sh} \quad \text{..................(1)}$$

Where:
I is the output current of the PV cell.
I_{ph} is the photo-generated current.
I_D is the current through the diode.
I_{sh} is the shunt leakage current.

In this study, we focus on designing and modeling a 213.15-Watt PV array, which serves as a fundamental building block for a solar energy system. The PV array consists of interconnected solar cells converting sunlight directly into electricity. The inputs of the **are solar Irradiance (G)**: Represents the intensity of sunlight incident on the PV array. It is measured in watts per square meter (W/m^2) [11]. Higher irradiance leads to higher photo-generated current and **Temperature (T)**: Represents the ambient temperature surrounding the PV array, typically measured in degrees Celsius (°C). Temperature affects the efficiency and output of the PV cells, as higher temperatures generally reduce efficiency. The outputs are **Voltage Output (V)**: Indicates the electrical voltage produced by the PV array. It is influenced by the irradiance and temperature, and **Power Output (P) for the ANN controller**: Indicates the amount of electrical power generated by the PV array. It is a product of the voltage and current generated by the PV cells [12-13].

The performance of the PV array under different conditions of solar irradiance and temperature is critical for understanding its operational capabilities. By simulating the PV array model under various conditions, we can predict its behavior and optimize its design for maximum efficiency [14].

The study focuses on the detailed modeling of a 213.15-Watt PV array, emphasizing its construction from p-n semiconductor junctions and its sensitivity to solar irradiance and temperature. The voltage and power outputs provide insights into the operational performance of the PV array, crucial for its application in renewable energy systems. Accurate modeling enables the AI prediction and enhancement of PV array performance in varying environmental conditions [15].

2.2. Modelling and Simulation of 213.15W PV Array

The PV array used in the designed PV system was selected from the MATLAB/Simulink toolbox for simulation purposes. Below is a detailed description of its electrical characteristics, as well as graphical representations of its performance under varying conditions of temperature and irradiance, Fig. 3, illustrates the PV array model selected from the MATLAB/Simulink toolbox, Table 1, show the electrical characteristics of the PV array model [16-17].

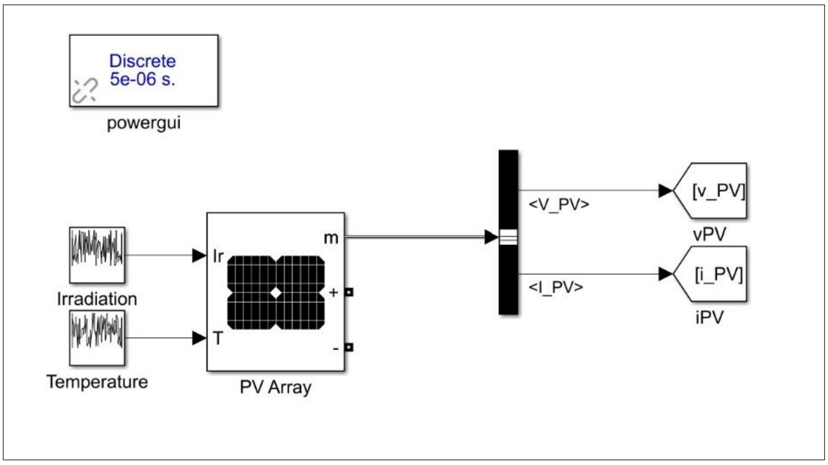

Figure 3 Block diagram for the proposed designed PV Array model

Table 1 Electrical characteristics of the pv module

Description	User-defined
Maximum power	312.15 W
Voltage at Pmax (Vmax)	29.00V
Current at Pmax (I_m)	7.35 A
Short Circuit current (I_{sc})	7.84 A
Open circuit voltage	36.30 V
Temperature coefficient Ki	0.102 A/°C

The Voltage-Current (V-I) characteristics curve illustrates the relationship between the voltage and the current output of the PV array at a specified temperature 25 °C, as seen in Fig. 4, this curve shows that the current remains relatively constant until the voltage reaches a certain point (near the open circuit voltage), after which the current drops sharply [18].

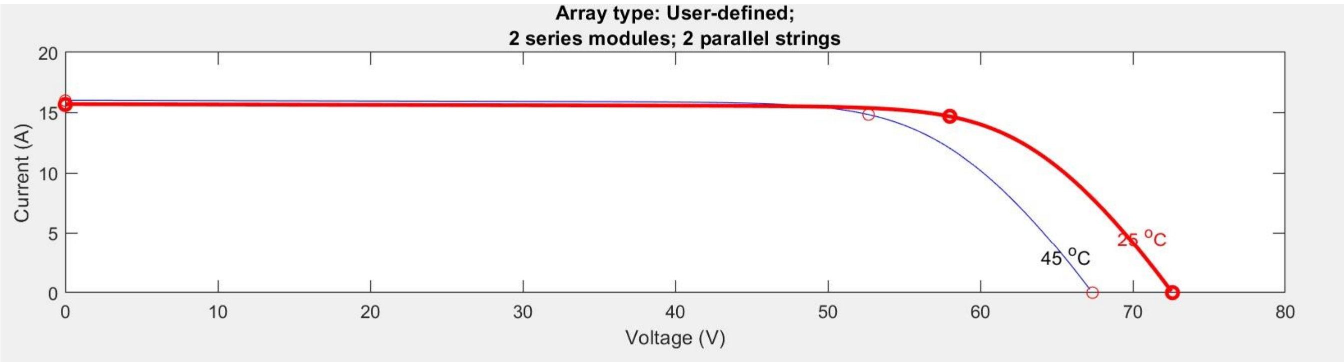

Figure 4 V-I characteristics curves of the PV array at a specified temperature

The Voltage-Power (V-P) characteristics curve displays how the power output of the PV array varies with the voltage at a specified temperature 25 °C, and 45 °C as seen in Fig. 5, this curve usually has a peak point representing the maximum power point (MPP), beyond which the power decreases with increasing voltage [19-20].

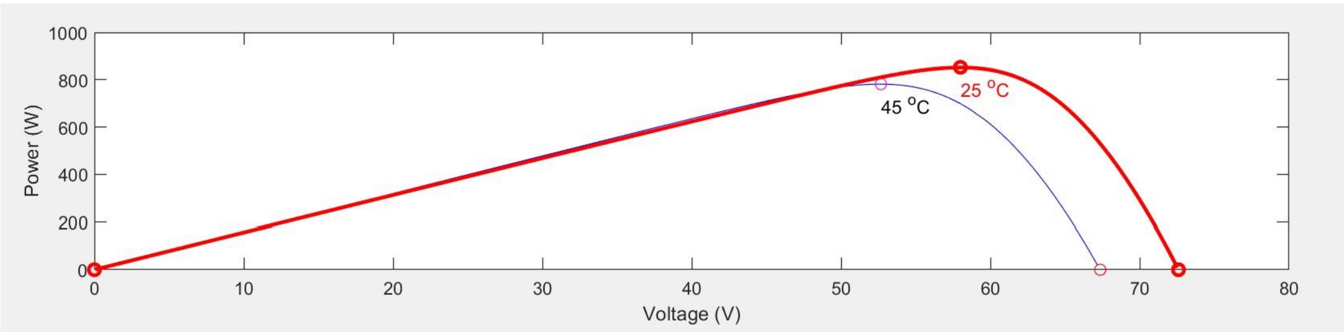

Figure 5 V-P characteristics curves of the PV array at a specified temperature

The Voltage-Current (V-I) characteristics curve at specified irradiance levels show how the output current varies with voltage under different sunlight intensities as seen in Fig. 6, Higher irradiance levels typically lead to higher current outputs while maintaining the general shape of the curve.

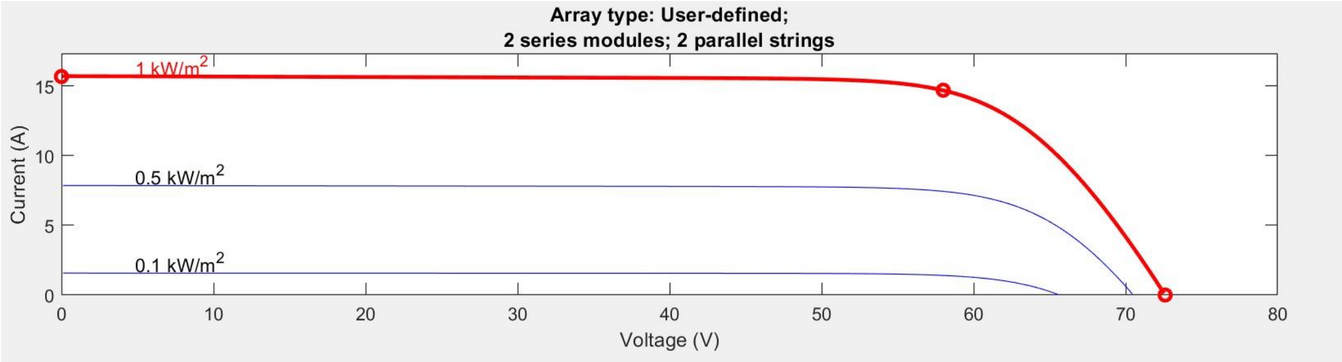

Figure 6 V-I characteristics curves of the PV array at a specified irradiance

The Voltage-Power (V-P) characteristics curve at specified irradiance levels depicts the variation in power output with voltage under different sunlight intensities. Like the temperature-dependent V-P curve as seen in Fig. 7, the irradiance-dependent curve also shows a peak at the maximum power point, with higher irradiance resulting in higher peak power values.

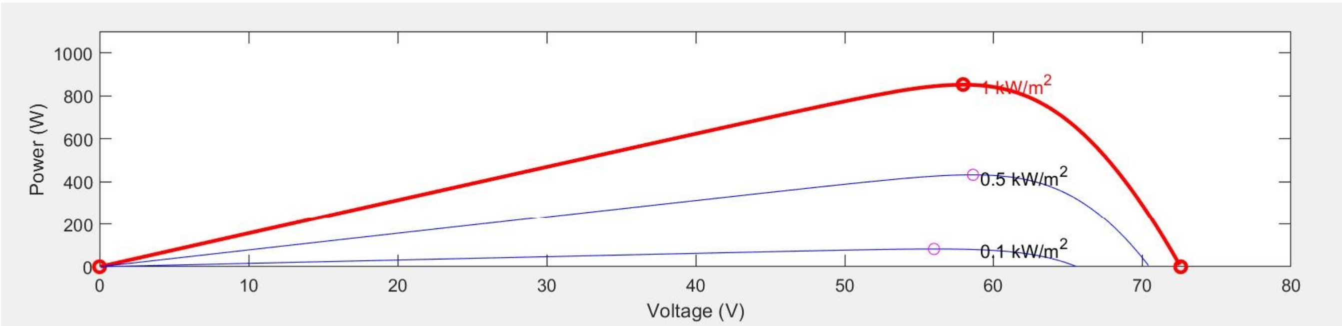

Figure 7 V-P characteristics curves of the PV array at a specified irradiance

2.3. Collecting Data:

To analyze the performance of the user-defined PV array, a comprehensive simulation was conducted using MATLAB/Simulink [21]. The goal was to examine how the PV array behaves under varying conditions of solar irradiance (G) and temperature (T), focusing on the maximum voltage (V_{max}) and maximum power (P_{max}) outputs. The data collected from these simulations are crucial for understanding the efficiency and operational characteristics of the PV array [22-23].

2.3.1. Simulation Parameters

- **Solar Irradiance (G)**: The intensity of sunlight incident on the PV array, measured in watts per square meter (W/m^2).
- **Temperature (T)**: The ambient temperature around the PV array, measured in degrees Celsius (°C).

2.3.2. Data Collection Process

- **Range of Conditions:** The PV array model was simulated across a broad range of solar irradiances and temperatures to ensure a comprehensive data set.
- **Simulink Simulation:** The simulations were performed in MATLAB/Simulink, leveraging the detailed PV array model from the toolbox.
- **Data Points:** A total of 104 data points were derived from the simulations, each corresponding to specific values of G and T. For each data point, Vmax and Pmax were recorded.

The results of the simulations, including the V_{max} and P_{max} values for the different conditions these data points provide valuable insights into the PV array's performance under various environmental conditions [24-25].

The collected data from the MATLAB/Simulink simulation offer a detailed view of the PV array's performance under different irradiance and temperature scenarios [26]. These insights are critical for optimizing the design and operation of PV systems in real-world applications. By understanding the relationship between environmental conditions and PV output, better predictions and enhancements can be made for renewable energy systems [27].

2.4. Converter Design and Operation

2.4.1. DC-DC Positive Output Super Lift Luo Converter Model

The DC - DC Positive Output Super Lift Luo converter is an advanced power electronics device designed to efficiently change and regulate the voltage level. It is particularly suitable for photovoltaic (PV) systems, where the unregulated and often low output voltage needs to be stepped up to a usable level [28].

2.4.2. Voltage Lift Technique:

- **Arithmetic Progression**: In basic voltage boosting configurations, the output voltage escalates incrementally, following a systematic arithmetic progression. This methodical increase ensures a predictable and orderly advancement in voltage levels, aligning with the sequential nature of arithmetic progressions commonly utilized in voltage conversion and control systems.
- **Geometric Progression**: The Positive Output Super Lift Luo converter, however, enhances this concept by achieving output voltage increases in a geometric progression. This results in a more significant and efficient voltage boost.

2.4.3. Components and Circuit Design

The converter consists of inductors, capacitors, diodes, and switches arranged in a specific configuration to achieve the desired voltage transformation.

The operation involves switching actions that control the energy storage and release in the inductors and capacitors, resulting in a step-up voltage at the output following an arithmetic progression [29-30].

Advantages Over Traditional Converters

- **Higher Voltage Gain**

Traditional converters like Boost, Cuk, and SEPIC can suffer from limited voltage gain. The Positive Output Super Lift Luo converter, on the other hand, offers a much higher voltage span due to its geometric progression mechanism [31].

- **Reduced Harmonics**

High harmonics are undesirable as they can cause interference and reduce the efficiency of the power system. The Positive Output Super Lift Luo converter minimizes harmonics, leading to a cleaner and more efficient power output.

- **Improved Power Factor**

Unwanted high-power factors in conventional converters can lead to inefficiencies. The Positive Output Super Lift Luo converter is designed to maintain a more desirable power factor.

- **Higher Efficiency**

The converter achieves higher efficiency by minimizing current ripples. Reduced ripple leads to lower losses and better performance of the overall system.

- **Higher Voltage Span**

The ability to achieve a higher voltage span makes this converter suitable for applications requiring substantial voltage boosts, such as connecting PV systems to external loads [32].

Practical Application in PV Systems

- **Unregulated PV Output**

PV systems typically produce an unregulated output voltage that can vary with changes in solar irradiance and temperature. This unregulated output is often insufficient for directly powering loads or integrating with the grid.

- **Voltage Regulation**

The Positive Output Super Lift Luo converter steps up the PV output voltage to a regulated level suitable for various applications. This regulation is crucial for ensuring that the power from the PV system is stable and usable [33].

Connection to External Loads

By using the Positive Output Super Lift Luo converter, the PV system can efficiently supply power to external loads. The converter ensures that the output voltage is within acceptable levels, enhancing the reliability and functionality of the PV system [34].

The Positive Output Super Lift Luo converter is designed with the following key components:

- **Switch**

Insulated Gate Bipolar Transistor (IGBT): A semiconductor switch used to control the duty cycle of the converter.

- **Diodes**

Regular Diode (D1, D2): Standard diodes used in the circuit to direct the current flow and prevent reverse current.

- **Energy Storage Components**

Inductors (L1): Used for energy storage and to smooth the current flow.

Capacitors (C1, C2): Used for energy storage and to smooth the voltage. Both capacitors have equal values (C2 = C1).

The converter is designed to ensure that the output voltage is always greater than the input voltage from the PV array. This is achieved through the positive output super lift technique, which steps up the output voltage in a geometric progression, maintaining positive values with respect to the input voltage [35].

The performance and behavior of the Positive Output Super Lift Luo converter can be described using the following equations:

Transfer Gain (K**)**: The transfer gain is defined as the ratio of the output voltage (Vo) to the input voltage (Vin).

$$V_o / V_{in} = (2 - K) / (1 - K) \ldots\ldots\ldots\ldots (2)$$

The relationship between the input voltage (Vin), output voltage (Vo), and transfer gain (K) is given by:

$$K = (2V_{in} - V_o) / (V_{in} - V_o) \ldots\ldots\ldots\ldots\ldots (3)$$

The output current can be calculated using Ohm's law. Given the load resistance (R), the output current (Io) is:

$$V_o = I_o R \ldots\ldots\ldots\ldots (4)$$

The DC-DC Positive Output Super Lift Luo converter is a sophisticated and efficient device for stepping up voltages in a non-inverting manner [36]. By using components such as IGBTs, diodes, inductors, and capacitors, it achieves high voltage gains and smooth, ripple-free outputs. The operational equations provided are essential for designing and analyzing the converter's performance in various applications, particularly in conjunction with PV systems [37-38].

The DC-DC Positive Output Super Lift Luo converter can be effectively understood through a block diagram, which provides a clear overview of its functional elements and the flow of electrical energy through the system. Here’s a detailed breakdown of the components and their interactions as depicted in Fig. 8 [39].

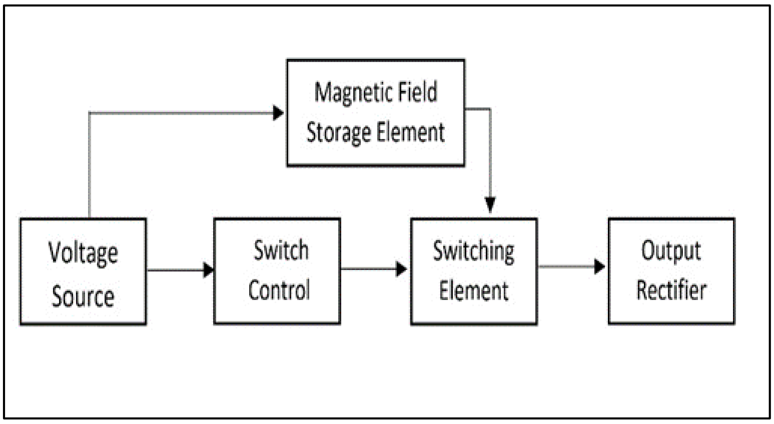

Figure 8 The Designed Block Diagram of a DC-DC Positive Output Super Lift Luo Converter

The block diagram components and descriptions:

- PV Array (Input Voltage Source)

The PV array generates a low and unregulated DC voltage because of converting sunlight into electrical energy this provides the input DC voltage to the converter.

- Switch Control

The component is an Insulated Gate Bipolar Transistor (IGBT), this block contains the control circuitry that manages the switching element. The switch control adjusts the duty cycle of the IGBT to regulate the energy transfer, it directs the action of the switching element to control the voltage conversion process [40].

- Magnetic Field Storage Element

The component is an Inductor (L1), that stores energy in its magnetic field during the switch-on period and releases it during the switch-off period, that smooths the current and helps boost the voltage.

- Capacitors (Energy Storage)

Two equal in value components, Capacitors (C1, C2), store and filter energy to provide a stable output voltage, resulting smoothing the voltage and reduce ripple, ensuring a consistent output [41-42].

- Diodes

The components are Diodes (D1, D2), they allow current to flow in one direction and prevent backflow, ensuring efficient energy transfer, resulting in direct current flow and contribute to voltage boosting.

- Output Rectifier and Filter

Consists of capacitors and additional diodes to ensure that the output voltage is smoothed and free of significant ripples, this provides a stable, high DC voltage to the load.

We can calculate from equation 3, the output voltage of the DC source with the voltage value $V_{pv} = 12V$, this voltage was sent to the input terminals of the DC-DC Positive Output Super Lift Luo converter, we will start our block diagram test with a duty cycle of 50%, the seen output voltage of the stepped-up value to be Vo = 34.44V, as seen from the designed simulation design in Fig. 4 [43-44].

Given the input voltage (Vpv = 12V) from the DC source and the duty cycle for the DC-DC Positive Output Super Lift Luo converter, we can use the provided information to calculate the expected output voltage (Vo = 34.44V).

From the equations provided earlier, the transfer gain (K) and the relationship between input and output voltages can be used to understand the conversion process.

$$K = (2V_{in} - V_{o)}) / (V_{in} - V_o)$$

$$K = (2 \times 12 - 34.44_{)}) / (12 - 34.44)$$

$$K = 0.465.$$

Now:

$$V_o / V_{in} = (2 - K) / (1 - K)$$

$$V_o / V_{in} = (2 - 0.465) / (1 - 0.465)$$

$$V_o / V_{in} \approx 2.87$$

$$V_o \approx 2.87 \times 12 \approx 34.44V.$$

This calculation confirms the observed output voltage of 34.44V for an input of 12V with a 50% duty cycle, demonstrating the correctness of the simulation results.

Fig. 9, illustrates the block diagram test setup and simulation results. The simulation confirms that with a 50% duty cycle, the input voltage of 12V from the DC source is successfully stepped up to 34.44V at the output of the Positive Output Super Lift Luo converter [45].

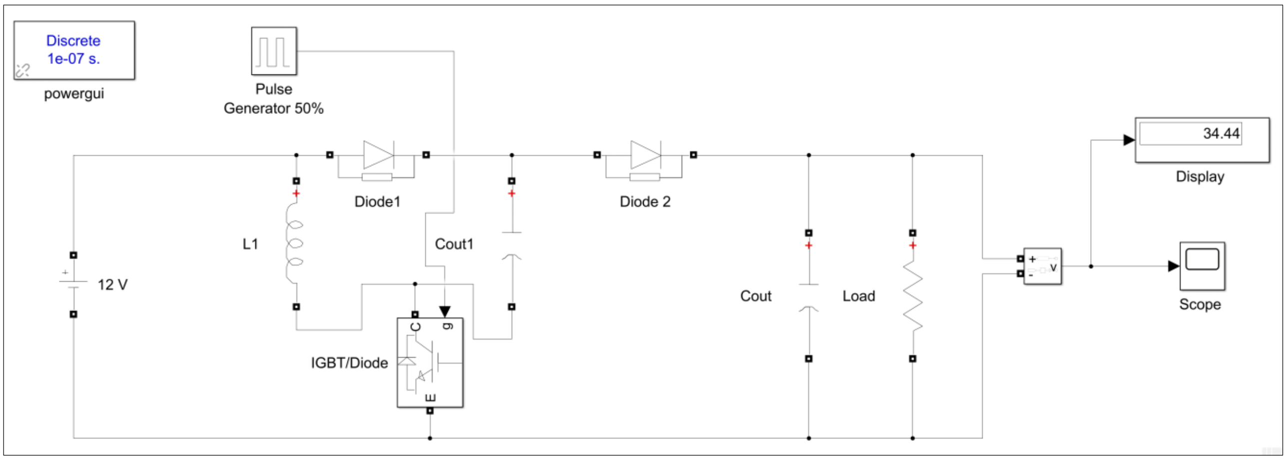

Figure 9 MATLAB\Simulink of 50% Duty Pulse Generator

The calculation and block diagram analysis align with the simulation results, verifying the performance of the Positive Output Super Lift Luo converter in stepping up the voltage from a DC source. This converter effectively increases the input voltage, providing a higher and regulated output voltage suitable for various applications [46].

The Positive Output Super Lift Luo converter proves to be highly efficient and effective for stepping up voltage levels. As seen in Fig. 10, the output voltage vs. time graph demonstrates its capability to achieve high voltage gains rapidly and stably, making it a superior choice compared to traditional converters like Cuk or Boost, which often suffer from overshoot and longer stabilization times. The converter's performance, as validated by both calculations and simulations, underscores its suitability for integrating PV systems with external loads requiring higher, regulated voltages [47].

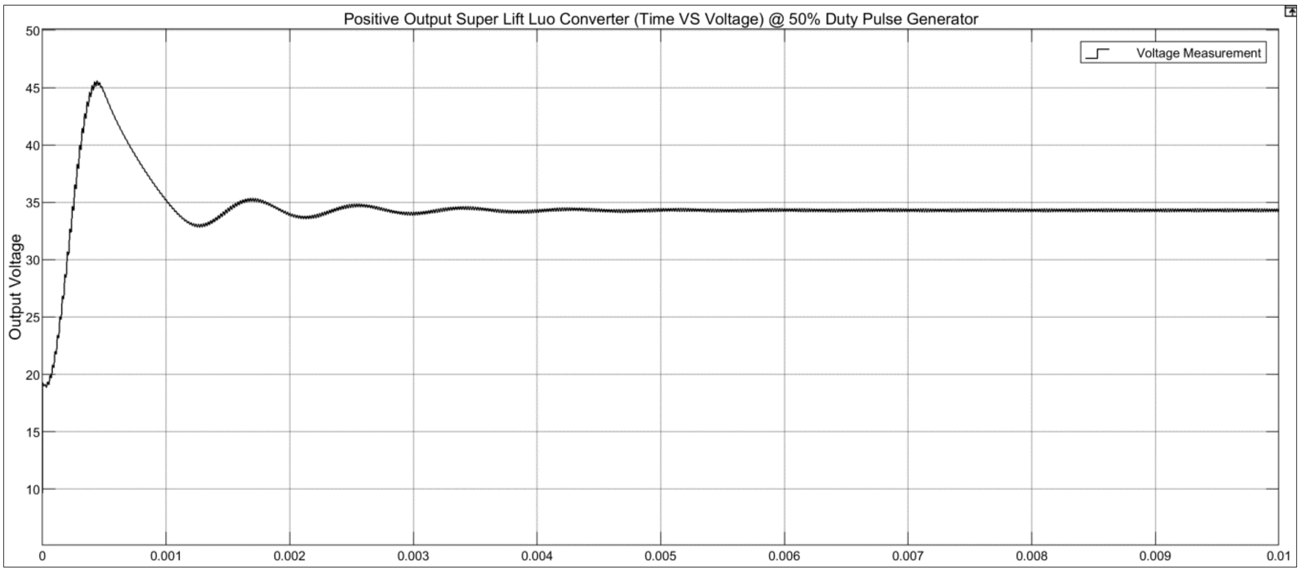

Figure 10 Positive Output Super Lift Luo Converter Time VS Voltage @ 50% Duty Pulse Generator

We can calculate from equation 3, the output voltage of the DC source with the voltage value $V_{pv} = 12V$, this voltage was sent to the input terminals of the DC-DC Positive Output Super Lift Luo converter, we will start our block diagram test with a duty cycle of 70%, the seen output voltage of the stepped-up value to be Vo = 50.56V, as seen from the designed simulation design in Fig. 11 [48].

Given the input voltage (Vpv = 12V) from the DC source and the duty cycle for the DC-DC Positive Output Super Lift Luo converter, we can use the provided information to calculate the expected output voltage (Vo = 50.56V).

From the equations provided earlier, the transfer gain (K) and the relationship between input and output voltages can be used to understand the conversion process.

$$K = (2V_{in} - V_{o}) / (V_{in} - V_{o})$$

$$K = (2 \times 12 - 50.56) / (12 - 50.56)$$

$$K = 0.688.$$

Now:

$$V_{o} / V_{in} = (2 - K) / (1 - K)$$

$$V_{o} / V_{in} = (2 - 0.688) / (1 - 0.688)$$

$$V_{o} / V_{in} \approx 4.21$$

$$V_{o} \approx 4.21 \times 12 \approx 50.52V.$$

This calculation confirms the observed output voltage of 50.56 for an input of 12V with a 70% duty cycle, demonstrating the correctness of the simulation results.

Fig. 11, illustrates the block diagram test setup and simulation results. The simulation confirms that with a 70% duty cycle, the input voltage of 12V from the DC source is successfully stepped up to 50.56V at the output of the Positive Output Super Lift Luo converter [49].

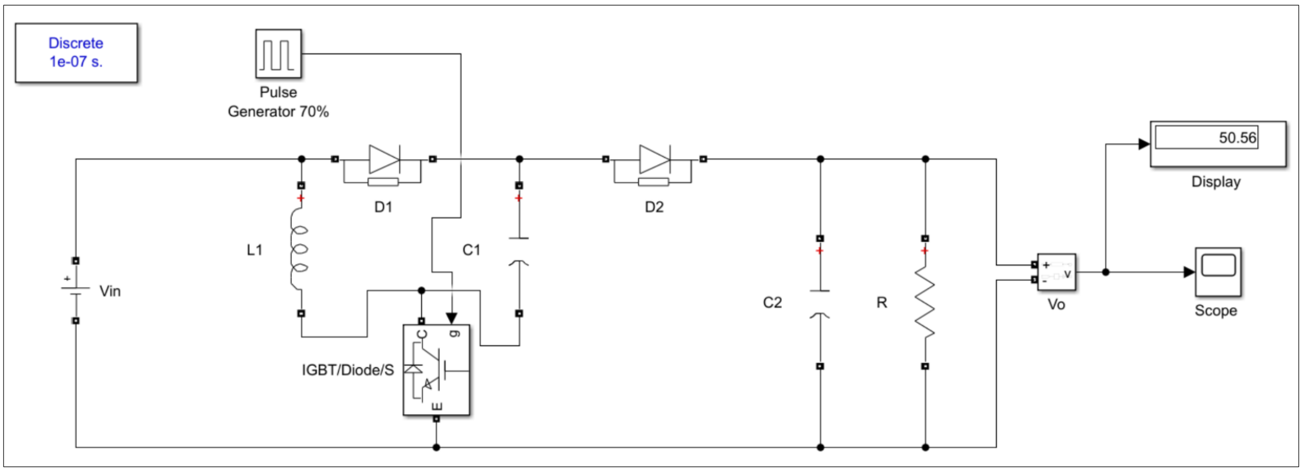

Figure 11 MATLAB\Simulink of 70% Duty Pulse Generator

The calculation and block diagram analysis align with the simulation results, verifying the performance of the Positive Output Super Lift Luo converter in stepping up the voltage from a DC source. This converter effectively increases the input voltage, providing a higher and regulated output voltage suitable for various applications [50].

The Positive Output Super Lift Luo converter proves to be highly efficient and effective for stepping up voltage levels. As seen in Fig. 12, the output voltage vs. time graph demonstrates its capability to achieve high voltage gains rapidly and stably, making it a superior choice compared to traditional converters like Cuk or Boost, which often suffer from overshoot and longer stabilization times. The converter's performance, as validated by both calculations and simulations, underscores its suitability for integrating PV systems with external loads requiring higher, regulated voltages [51].

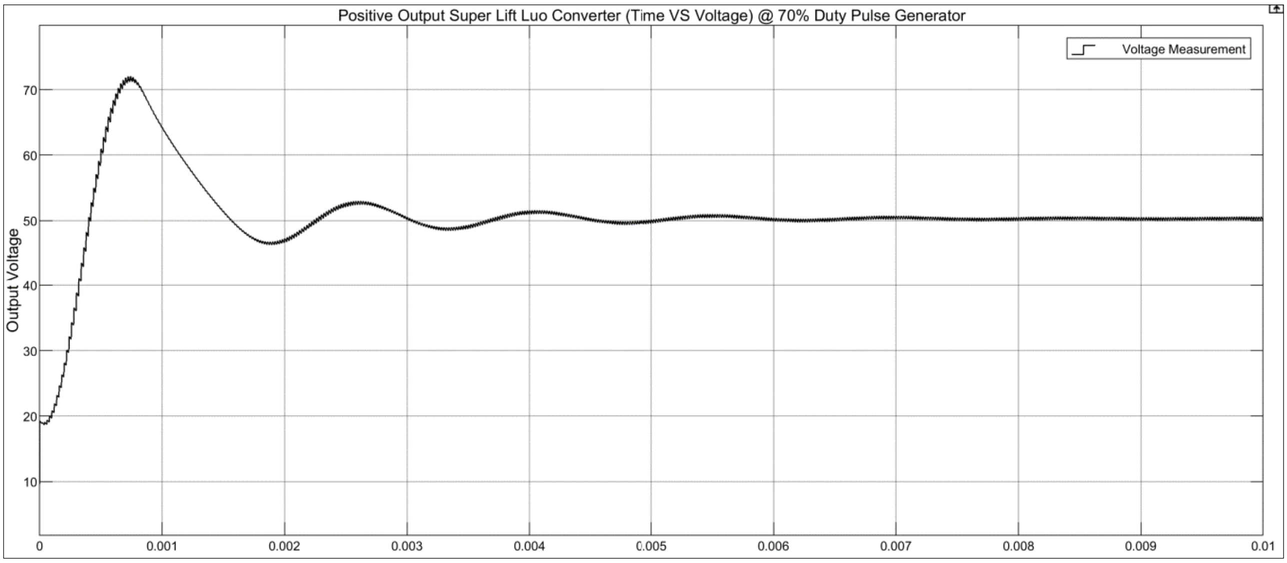

Figure 12 Positive Output Super Lift Luo Converter Time VS Voltage @ 70% Duty Pulse Generator

3. Artificial neural network (ANN)

To enhance the performance and efficiency of the photovoltaic (PV) system, Artificial Intelligence (AI) controllers are increasingly being integrated. One effective AI approach is the use of Artificial Neural Networks (ANNs) to track the Maximum Power Point (MPP) of the PV array.

The ANN employed in this proposed design utilizes the Levenberg-Marquardt algorithm to solve its equations. This algorithm is chosen for its efficiency and accuracy in solving complex nonlinear least-squares problems. Here's a detailed description of how the ANN is set up and utilized in the PV system:

3.1. ANN Structure and Training

3.1.1. Input Variables

- **Solar Irradiance (G)**: Represents the intensity of sunlight incident on the PV array.
- **Temperature (T)**: Represents the ambient temperature affecting the PV array.

3.1.2. Network Architecture

The ANN consists of three layers: input layer, hidden layer, and output layer.

- **Input Layer**: Receives inputs G and T.
- **Hidden Layers**: Contains 10 neurons, designed to capture the nonlinear relationships between the inputs and outputs. The exact number of hidden layers can vary, but 10 neurons in the hidden layers have been chosen for this design.
- **Output Layer**: Provides the outputs, which are the predicted values for maximum power (Pmax) and maximum voltage (Vmax).

3.1.3. Training Algorithm

Levenberg-Marquardt Algorithm: This algorithm is used due to its capability to handle the non-linearities and complex relationships in the data. It is faster and more accurate compared to other training algorithms, making it suitable for real-time applications. The training involves adjusting the weights and biases of the network to minimize the error between the predicted and actual MPP values [52].

MATLAB/Simulink is used for the simulation and training of the ANN. The neural network is trained with a dataset that includes various combinations of solar irradiance and temperature values, ensuring the network can generalize well to new, unseen data.

3.2. Selecting the Artificial Neural Network (ANN) Structure

In our proposed design, the ANN is employed to track the Maximum Power Point (MPP) of the PV array, utilizing the inputs of irradiance (G) and temperature (T). The ANN structure and its connection to the PV system are detailed as follows:

- Input Layer: Consists of two neurons, representing the inputs: Solar Irradiance (G) and Temperature (T).
- Output Layer: Consists of two neurons, representing the outputs: Voltage (V) and Power (P).
- Hidden Layer: Contains a specified number of neurons, connected to the input and output layers through weighted interconnections. The number of neurons in the hidden layer significantly influences the network's ability to capture the nonlinear relationships between inputs and outputs.
- Network Training: Training Algorithm: Levenberg-Marquardt algorithm, known for its efficiency and accuracy in solving complex nonlinear problems. Training Method: Trial-and-error approach is used to determine the optimal number of neurons in the hidden layer. The ANN is trained using a dataset comprising various combinations of irradiance (G) and temperature (T), ensuring robust performance across different operating conditions [53].
- Weighted Interconnections: The inputs (G and T) are connected to the neurons in the hidden layer through weighted connections. These weights are adjusted during the training process to minimize the error in predicting the output values (V and P).
- Prediction of Outputs: The trained ANN processes the input values and calculates the corresponding voltage (V) and power (P). This prediction allows the PV system to operate at its maximum efficiency by continuously adjusting to the MPP. This enabled the generation of the required duty cycle for the DC-DC Positive Output Super Lift Luo converter, which controlled the Insulated Gate Bipolar Transistor (IGBT) switch. This process ensured the maximum harvesting of renewable energy by adjusting the PV system voltage and matching the PV and load resistances.
- Influence of Hidden Layers: The performance of the ANN depends on the architecture, specifically the number of hidden layers and the number of neurons in each layer. Through trial and error, the optimal configuration is found to achieve high accuracy and fast response times. The influence of hidden layers in ANN architectures for PV systems is pivotal in achieving high-performance MPPT. By carefully configuring the number of hidden layers and neurons per layer through iterative testing, we can optimize the network's accuracy, response speed, and overall efficiency in extracting maximum power from solar energy. This approach not only enhances the

reliability and performance of PV systems but also advances the adoption of renewable energy technologies in practical applications.

- Simulation Setup: The ANN is implemented in MATLAB/Simulink, where it is trained and tested using the Levenberg-Marquardt algorithm. Fig. 13, illustrates the structure of the ANN, showing the input layer with two neurons (G, T), the hidden layer with an optimized number of neurons, and the output layer with two neurons (V, P). The implementation of an ANN for optimizing PV systems exemplifies a sophisticated approach to MPPT. By structuring the ANN with an optimized number of neurons in the hidden layer and training it with relevant datasets using the Levenberg-Marquardt algorithm, we can enhance the system's ability to maximize energy output under changing environmental conditions. This setup not only improves the efficiency of PV systems but also demonstrates the practical application of AI techniques in renewable energy technologies. MATLAB/Simulink provides a graphical environment for designing, simulating, and analyzing dynamic systems, including neural networks. This environment facilitates the integration of the ANN model with other components of the PV system, such as the MPPT algorithm and the DC-DC converter. After training, the ANN model is tested to evaluate its performance in predicting voltage (V) and power (P) outputs under various combinations of solar irradiance and temperature. The accuracy and efficiency of the ANN in tracking the Maximum Power Point (MPP) directly influence the overall energy harvesting efficiency of the PV system.

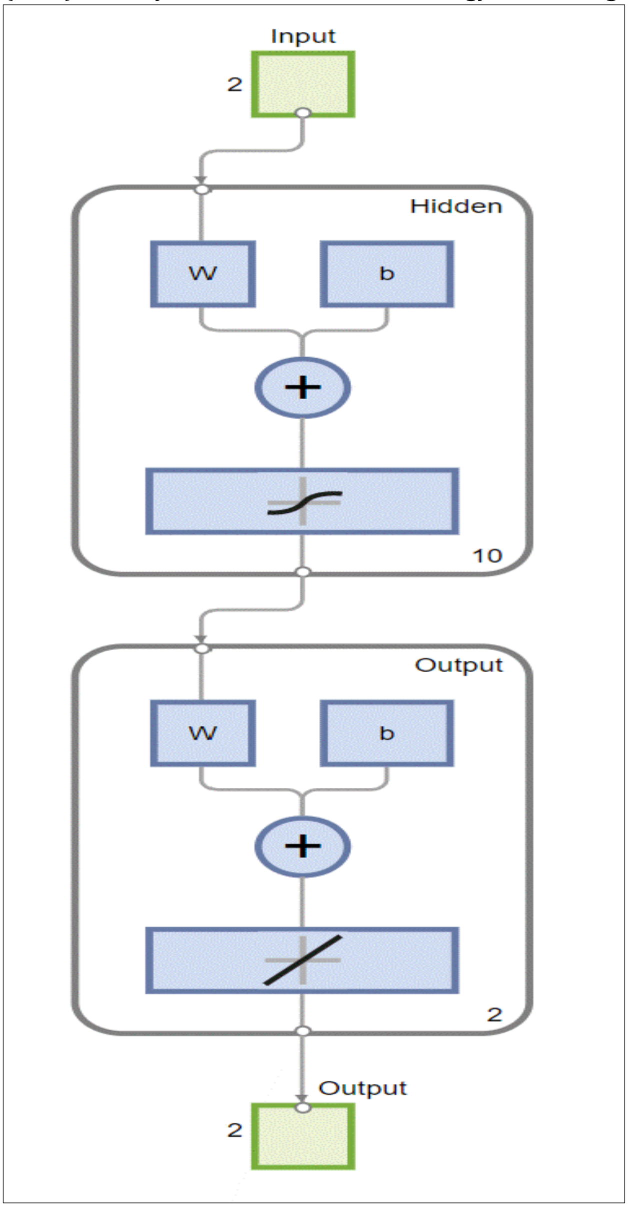

Figure 13 Proposed ANN structure

The integration of an ANN for MPP tracking in PV systems represents a significant enhancement in system performance. By accurately predicting the maximum power point through inputs of irradiance and temperature, the ANN ensures optimal operation of the PV array. The trial-and-error method used to train the ANN, coupled with the Levenberg-Marquardt algorithm, provides a robust and efficient solution for handling the nonlinear characteristics of the PV system. Implementing this in MATLAB/Simulink allows for detailed simulation and testing, ensuring reliable performance in real-world applications.

To ensure that the ANN controller for MPP tracking in the PV system is optimally trained and performs efficiently, a comprehensive comparison was conducted using different random data sample sets. The goal was to identify the best random sample data set choice to achieve the highest efficiency in tracking the MPP. The sample sets used in the comparison included 104, 201, and 1001 random data points.

3.3. Data Sample Sets

3.3.1. 104 Random Data Samples:

This initial data set was used to train the ANN controller. It included various combinations of irradiance (G) and temperature (T) values, covering a broad range of operating conditions.

3.3.2. 201 Random Data Samples:

An expanded data set aimed at providing more variability and potentially improving the training accuracy and generalization of the ANN.

3.3.3. 1001 Random Data Samples:

A significantly larger data set intended to capture even more variability in the inputs, allowing the ANN to learn more intricate patterns and relationships between the inputs (G and T) and the outputs (V and P).

After training the ANN controller with each of the three data sets, their performance was compared based on the following criteria:

- Accuracy

The precision of the ANN controller in predicting the maximum power point (MPP) for given irradiance and temperature values.

- Efficiency

The overall efficiency of the PV system when using the ANN controller to track the MPP. The PV system can achieve maximum energy harvesting and improved performance, contributing to more efficient and sustainable solar energy utilization.

- Generalization

The ability of the ANN controller to perform well on new, unseen data points, reflecting its robustness and adaptability.

The comparison of the three data sets (104, 201, and 1001 random samples) with 91.0380% for 104 samples, 91.8293% for 201 samples, and 92.6218% for 1001 samples revealed that the ANN controller trained with the 1001 random data samples achieved the best performance. This larger data set allowed the ANN to learn more detailed patterns and provided superior accuracy and efficiency in tracking the MPP.

By training the ANN with a comprehensive and diverse data set, the PV system's performance was significantly enhanced. The ANN controller trained with 1001 data samples emerged as the optimal choice for achieving the highest efficiency in the PV system, demonstrating robust and reliable performance across various operating conditions.

Based on these findings, the ANN controller trained with 1001 random data samples was implemented in the PV system. This ensured that the system could reliably track the MPP, maximize power output, and operate efficiently under diverse environmental conditions. The use of MATLAB/Simulink for simulation and training provided a robust framework for developing and testing the ANN controller, ensuring its effectiveness in real-world applications.

4. Recurrent neural network (RNN)

To further enhance the efficiency of the PV system, a Recurrent Neural Network (RNN) was introduced. The RNN's unique architecture, which includes feedback connections within its inner layers, makes it particularly suitable for handling time-dependent data and nonlinear input variations. This feature is critical for tracking the maximum power point (MPP) in real-time, ensuring optimal performance of the PV array.

4.1. Feedback Mechanism

Unlike traditional feedforward neural networks, RNNs have loops that allow information to be passed from one step to the next. This feedback mechanism helps the network maintain context over sequences of input data, making it ideal for handling the dynamic and nonlinear nature of PV system inputs.

4.2. Training Algorithm:

The RNN is trained using the Mean Squared Error (MSE) algorithm. MSE is a standard approach for regression problems, minimizing the average of the squares of the errors between predicted and actual values. MATLAB/Simulink is used to implement and train the RNN, leveraging its advanced capabilities for handling complex simulations and AI training.

4.3. RNN Architecture

- **Input Layer**: The RNN receives two input variables: Solar Irradiance (G) and Temperature (T).
- **Hidden Layers**: The RNN consists of 4 hidden layers, each containing 10 neurons. The feedback connections within these layers allow the network to capture temporal dependencies and nonlinear relationships in the data.
- **Output Layer:** The network produces one output: Voltage (V), which correspond to the maximum power point (MPP) parameters.

Accuracy: The RNN is expected to provide higher accuracy in predicting the MPP due to its ability to handle nonlinear and time-dependent input variations effectively. PV systems exhibit nonlinear behavior due to the complex interactions between solar irradiance (G), temperature (T), and the resulting electrical characteristics (voltage and current). RNNs are adept at capturing these nonlinear relationships through their recurrent connections, which allow them to retain information over time and process sequences of inputs effectively.

Response Time: The incorporation of RNNs in PV systems offers significant advantages in terms of response time compared to traditional controllers like ANNs. By leveraging their recurrent nature and ability to process temporal data effectively, RNNs enable faster adaptation to change in irradiance and temperature. This capability is instrumental in maximizing energy harvesting efficiency and ensuring robust performance of PV installations across diverse environmental conditions. Thus, RNNs represent a promising technology for advancing the reliability and effectiveness of renewable energy systems.

Efficiency: The integration of technologies such as RNNs in PV systems results in significant efficiency gains. By enhancing accuracy in MPP tracking and enabling faster responses to environmental changes, RNNs optimize energy harvesting and increase overall system efficiency. This not only improves the economic viability of PV installations but also supports environmental sustainability by maximizing renewable energy utilization. Thus, RNNs represent a pivotal advancement in advancing the capabilities and reliability of solar PV technology.

4.4. Develop and Train the RNN

As seen in Fig. 14, utilizing MATLAB/Simulink to develop the RNN model, incorporating the necessary feedback mechanisms and hidden layers. Train the RNN using a comprehensive data set of irradiance and temperature values, optimizing the network with the MSE algorithm.

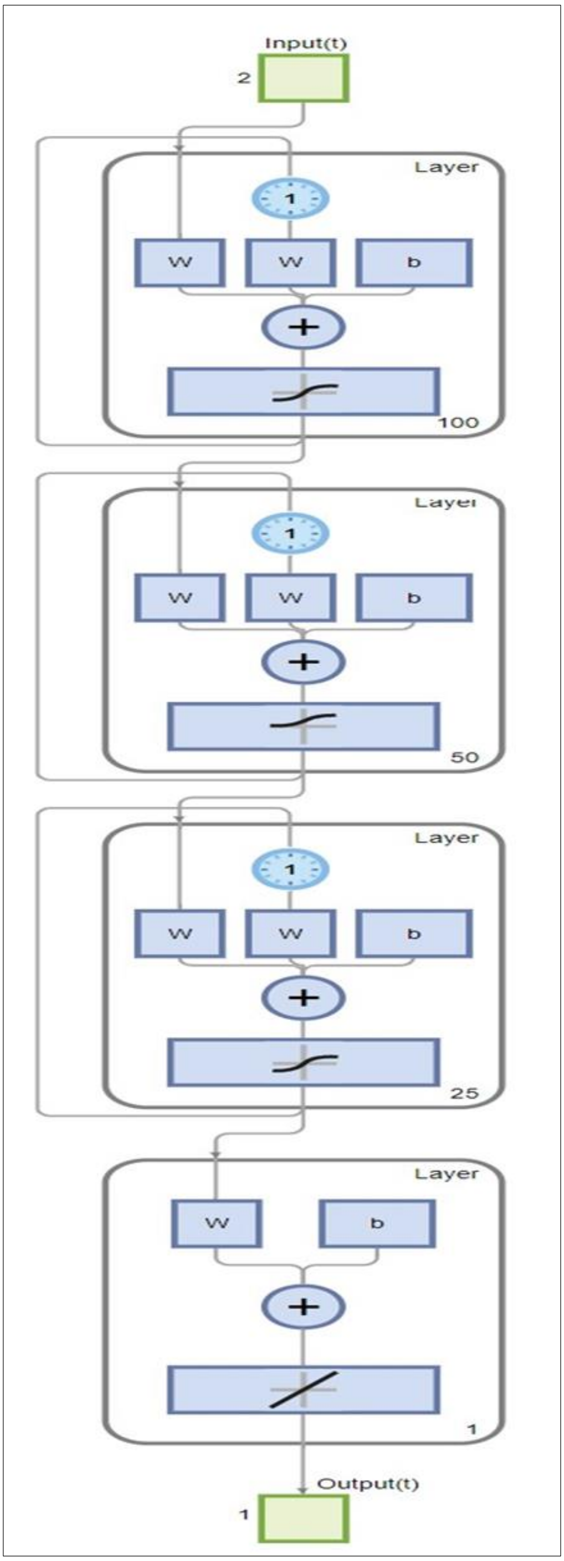

Figure 14 Proposed RNN structure

The introduction of an RNN for MPP tracking in the PV system represents a significant advancement in achieving higher efficiency. The feedback mechanism within the RNN's inner layers allows it to handle the nonlinear and time-dependent nature of the input variables more effectively than traditional ANNs.

By leveraging the RNN's capabilities and training it with the MSE algorithm in MATLAB/Simulink, the PV system can achieve more precise and reliable MPP tracking. This results in optimal performance, maximizing the power output and overall efficiency of the PV array under diverse and dynamic environmental conditions.

To ensure the optimal training and performance of the Recurrent Neural Network (RNN) controller for Maximum Power Point (MPP) tracking in the PV system, a comprehensive comparison was conducted using different random data sample sets. The goal was to determine the most effective sample size for achieving the highest efficiency in MPP tracking. The sample sets included in the comparison were 104, 201, and 1001 random data points.

4.5. Data Sample Sets

4.5.1. 104 Random Data Samples

This initial data set represents a smaller sample size, which provides a quick training process but may limit the network's ability to generalize well to new data points.

4.5.2. 201 Random Data Samples

A medium-sized data set that offers a balance between training time and generalization capability, potentially improving the network's performance over the smaller data set.

4.5.3. 1001 Random Data Samples

A large data set that encompasses a wide range of input conditions, allowing the RNN to learn more detailed patterns and relationships, potentially leading to higher accuracy and efficiency.

The RNN controller was trained using the Mean Squared Error (MSE) algorithm in MATLAB/Simulink for each of the three data sample sets. Each training session involved adjusting the network's weights and biases to minimize the error in predicting the output voltage (V) for given input values of irradiance (G) and temperature (T), RNN performance was compared based on the following criteria:

- **Accuracy**

The precision of the RNN controller in predicting the MPP for varying input conditions of irradiance and temperature.

- **Efficiency**

The overall efficiency of the PV system when using the RNN controller to track the MPP, measured by the maximum power output achieved.

- **Generalization**

The ability of the RNN controller to perform well on new, unseen data points, reflecting its robustness and adaptability.

The comparison of the three data sample sets (104, 201, and 1001 random samples) with 84.4452% for 104 samples, 92.6921% for 201 samples, and 93.2652% for 1001 samples revealed that the RNN controller trained with 1001 random data samples achieved the best performance. This larger data set enabled the RNN to learn more intricate patterns and provided superior accuracy and efficiency in tracking the MPP.

By training the RNN with a comprehensive and diverse data set, the PV system's performance was significantly enhanced. The RNN controller trained with 1001 data samples emerged as the optimal choice for achieving the highest efficiency in the PV system, demonstrating robust and reliable performance across various operating conditions.

Based on these findings, the RNN controller trained with 1001 random data samples was implemented in the PV system. This ensured that the system could reliably track the MPP, maximize power output, and operate efficiently under diverse environmental conditions. The use of MATLAB/Simulink for simulation and training provided a robust framework for developing and testing the RNN controller, ensuring its effectiveness in real-world applications.

5. Results and discussion for artificial neural network vs recurrent Neural network

As seen in Table 2, with the use of a P&O controller, we got an efficiency reaching 91.2649%, inserting an ANN controller with 104 samples the efficiency was 91.0380%, for 201 samples it reached 91.8293%, and 92.6218% for 1001 samples which is higher compared to inserting a P&O controller. The jump from 104 to 1001 samples showed a significant improvement, indicating the importance of a larger and more diverse data set for training the ANN controller effectively. The integration of ANN controllers, especially when trained with larger sample sizes, significantly enhances the efficiency of PV systems compared to conventional P&O controllers. The results demonstrate the effectiveness of AI techniques in maximizing power output and improving overall system performance under varying environmental conditions. Using an ANN controller for MPP tracking in a PV system substantially enhances overall efficiency compared to the traditional P&O method. The efficiency gains are more pronounced with larger training sample sizes, demonstrating the ANN's capability to more accurately predict and track the MPP under varying environmental conditions.

Table 2 Comparison of all used ANN controllers

No.	Controller Type	Efficiency
1	No controller	80.7254%
2	P&O	91.2649%
3	ANN using 104 Random samples	91.0380%
4	ANN using 201 Random samples	91.8293%
5	ANN using 1001 Random samples	92.6218%

As seen in Table 3, with the use of a P&O controller, we got an efficiency reaching 90.8239%, inserting an RNN controller with 104 samples decreased the efficiency to 87.4452%, 92.6921% for 201 samples, and 93.2652% for 1001 samples which is higher compared to inserting a P&O controller. The jump from 104 to 1001 samples showed a significant improvement, indicating the importance of a larger and more diverse data set for training the RNN controller effectively. The integration of RNN controllers, especially when trained with larger sample sizes, significantly enhances the efficiency of PV systems compared to conventional P&O controllers. The results demonstrate the effectiveness of AI techniques in maximizing power output and improving overall system performance under varying environmental conditions. Using an RNN controller for MPP tracking with a DC – DC Positive Output Super Lift Luo converter in a PV system can significantly enhance overall efficiency compared to the traditional P&O method, particularly with larger training sample sizes. The results demonstrate the RNN's capability to more accurately predict and track the MPP under varying environmental conditions, though careful consideration of training data size is crucial.

Table 3 Comparison of all used RNN controllers

No.	Controller Type	Efficiency
1	No controller	80.7254%
2	P&O	90.8239%
3	ANN using 104 Random samples	87.4452%
4	ANN using 201 Random samples	92.6921%
5	ANN using 1001 Random samples	93.2652%

6. Conclusion

In our work, we successfully designed and implemented AI-based ANN and RNN controllers using MATLAB/Simulink to optimize a photovoltaic (PV) system. We developed and compared ANN and RNN controllers with various sample sizes and integrated them into a PV system employing a DC-DC Positive Output Super Lift Luo converter. This converter boosts the PV array voltage and ensures impedance matching with load resistances. The AI controllers were designed to predict the maximum output voltage based on varying irradiance (G) and temperature (T) inputs, which change nonlinearly, necessitating sophisticated predictive algorithms. The predicted maximum output voltage from the AI controllers was fed into the Maximum Power Point Tracking (MPPT) system, enabling the generation of the required duty cycle for the converter, which controlled the Insulated Gate Bipolar Transistor (IGBT) switch. The RNN controller demonstrated superior accuracy and efficiency compared to the ANN controller, particularly with a sample size of 1001 points. Increasing the sample size for training the RNN controller significantly enhanced its efficiency. Future research could focus on testing with larger datasets, exploring different architectures, and implementing the AI controllers in real-world PV systems to validate their performance under actual environmental conditions. This work highlights the potential of AI in enhancing renewable energy system efficiency and reliability, paving the way for more advanced PV system designs.

Compliance with ethical standards

Acknowledgments

I acknowledge the contributions made by my co-author and those who supported us during our research.

Disclosure of conflict of interest

The authors declare that no conflict of interest exists between them.

References

[1] K. Mohammad and S. M. Musa, "Optimization of Solar Energy Using Artificial Neural Network Controller," 2022 14th International Conference on Computational Intelligence and Communication Networks (CICN), Al-Khobar, Saudi Arabia, 2022, pp. 681-685, doi: 10.1109/CICN56167.2022.10008271.

[2] K. A. Mohammad and S. M. Musa, "Optimization of Solar Energy Using Recurrent Neural Network Controller," 2022 14th International Conference on Computational Intelligence and Communication Networks (CICN), Al-Khobar, Saudi Arabia, 2022, pp. 1-6, doi: 10.1109/CICN56167.2022.10041248.

[3] H. Ibrahim, and N. Anani, "Variations of PV module parameters with irradiance and temperature," Energy Procedia, 2017.

[4] K. Razieh, and M. Hamiruce, "Comparison of ANN and P&O MPPT methods for PV applications under changing solar irradiation," IEEE, 2013.

[5] A. Mellit, S. Kalogirou, "Artificial Intelligence techniques of sizing photovoltic systems," Renewable Sustainable Energy, 2019.

[6] M. Patil and A. Deshpande, "Design and simulation of perturb and observe Maximum Power Point Tracking in MATLAB and Simulink," ICSTM, 2015.

[7] K. Jobeda, F. Simon, "Modeling of photovoltaic array in MATLAB Simulink and maximum power point tracking using neural network," Electrical & Electronic Technology Open Access Journal, 2018.

[8] K. Ishaque and Z. Salam, " A review of Mazimum Power Point Tracking techniques of PV system for uniform insolation and partial shading condition," Renewable Sustainable Energy Rev, 2013.

[9] A. Nasrudin, P. Rahim, "Photovoltaic module modeling using Simulink/Matlab," International Conference on Sustainable Future for Human Security, 2012.

[10] M. Samiul, and M. Kamrul, "Design and simulation of maximum poer point traching of photovoltaic system using ANN," ICEEICT, 2016.

[11] P. Sahu, and S. Nema, "Physical design and modelling of boost converter for maximum power point traching in solar PV systems," ICEPES, 2016.

[12] N. Patcharaprakiti, S. Premrudeepchacharn, "Maximum Power Point Tracking Using Adaptive Fuzzy Logic Control for Grid-Connected Photovoltaic System," IEEE, 2002.

[13] S. Azadeh, M. Saad, "Simulation and Hardware Implementation of Incremental Conductance MPPT With Direct Control Method Using Cuk Converter," IEEE, 2011.

[14] B. Mark, "Neural Network Toolbox for Use with MATLAB," Book, 2004.

[15] G. Kevin, "An introduction to neural networks," Book, 1997.

[16] F. Kulsoom, A. Mohammad, "Optimization of Solar Energy Using ANN Techniques," International Conference on Power Energy, 2019.

[17] R. Hegazy, "A new MATLAB/Simulink model of triple-junction solar cell and MPPT based on artificial neural networks for photovoltaic energy systems," Ain Shams Engineering Journal, 2015.

[18] G. Yu, J Choi, and G. Kim, "A novel two-mode MPPT control algorithm based on comparative study of existing algorithms," Solar Energy, 2004.

[19] M. Malik, R Kamara, "A Novel PV based ANN Optimization Converter for off grids Locomotives," ICTAI, 2021.

[20] H. Madvar, M Dehghani, and R. Memarzadeh, "Derivation of Optimized Equations for Estimation on Dispersion Coefficient in Natural Stream Using Hybridized ANN With PSO and CSO Algorithms," IEEE, 2020.

[21] M. Manimegalai, K. Sebasthiarani, "Efficient Routing in Smart Grid Communication by Secured ABC – ANN Algorithm," IEEE, 2022.

[22] H. Elaissaoui, Z. Zerouali, "MPPT Algorithm Based on Fuzzy Logic and Artificial Neural Network (ANN) for a Hybrid Solar/Wide Power Generation System," IEEE, 2020.

[23] T. Nguyen, M. Pham, and T. Duong, "A Recent Invasion Wave of Deep Learning in Solar Power Forecasting Techniques Using ANN," IEEE, 2021.

[24] O. Savchenko, O. Miroshnyk, "Improving the Efficiency of Solar Power Plants Based on Forecasting the Intensity of Solar Radiation Using Artificial Neural Networks," IEEE, 2021.

[25] N. Shyni, M. Linda, "An efficient maximum power point tracking in hybrid solar and wind energy system: A combined AMD-RNN technique," Journal of Intelligent & Fuzzy Systems, 2019.

[26] N. Mpho, H. Ali, "Comprehensive Evaluation of Machine Learning MPPT Algorithms," Jornal of Electrical Engineering & Technology, 2020.

[27] F. Hassan, E. Ali, "Dynamic global power extraction from partially shaded photovoltaic using deep recurrent neural network and improved PSO techniques," WILEY, 2018.

[28] S. Padmanaban, O. Mohammad, "LSTM Recurrent Neural Network Classifier for High Impedance Fault Detection in Solar PV Integrated Power System," IEEE Access, 2021.

[29] N. Mpho, H. Ali, "Commensurate Evaluation of Suppoer Vector Machine and Recurrent Neural Network MPPT Algorithm for a PV system under different weather conditions," IEEE, 2020.

[30] K. Sudarsan, G. Sreenivasan, "Power Quality Enhancement in Grid Connected Hybrid PV/WT System using Tree Seed Algorithm with RNN," Helix, 2020.

[31] V. Kumar, M. Patowary, "Solar Plant Integration to Utility Grid with Improved Power Quality by using RNN-Hebbian-LMS Current Controller," IEEE, 2018.

[32] R. Pascanu, T. Mikolov, "On the difficulty of training recurrent neural networks," International Conference on Machine Learning, 2013.

[33] L. Sindhura, K. Chaudhary "Artificial Neural Network Implementation for Maximum Power Point Traching of Optimized Solar Power Panel," 2016

[34] R. Das, "Application of Recurrent Neural Network using MATLAB SIMULINK in Medicine," Italian Journal of Pure and Applied Mathematics, 2018.

[35] Y. Zhang, G. Xiaojiao "MATLAB Simulink Modeling and Simulation of Zhang Neural Network for Online Time-Varying Matrix Inversion," IEEE, 2008.

[36] G. Tina, C. Ventura "A State-of-Art-Review on Machine-Learning Based Methods for PV," Applied Science, 2021.

[37] A. Toure, D. Tchoffa "Modeling and Control Maximum Power Point Traching of an Autonomous Photovoltaic System Using Atrificial Intelligence," Energy and Power Engineering, 2021.

[38] M. Mohamed, C. Ines "A Novel Approach Based Deep RNN Using Hybrid NARX-LSTM Model For Solar Power Forecasting," Aexiv, 2019.

[39] M. Nkambule, A. Hasan, A, Ali "Comprehensive Evaluation of Machine Learning MPPT Algorithms for PV Systems Under Different Weather Conditions," JEET 2020.

[40] N. Mohan, Department of Electrical and Computer Engineering – University of Minnesota, "First Course on Power Electronics and Drives," 2003.

[41] M. Patil, "Modelling and simulation of dc drive using PI and PID controller," International Journal of Innovative Research in Electrical, Electronics, Instrumentation and Control Engineering, vol. 2, pp. 1-15, 2014.

[42] N. Ismail, K. Zakaria, N. Nazar, and M. Syaripuddin, "DC motor speed control using a fuzzy logic controller," In AIP Conference Proceedings, vol. 1930, pp. 020026, 2018.

[43] M. Ahmad, R. Pankaj, M. Anito, and M. Megha, "Speed Control of a D Motor Using Fuzzy Logic Application," International Journal of Research in Engineering, Technology and Science, vol. 7, pp. 3011, 2018.

[44] A. Ahmed, A. Kabir, and M. Shahjahan, IEEE. "Speed control of DC motor with FZ-D controller," 3rd International Conference on Electrical Information and Communication Technology (EICT), pp. 1-6, 2017.

[45] K. Passino, S. Yurkovich, and M. Reinfrank, "Fuzzy control," Menlo Park, CA: Addison-Wesley, vol. 42, pp. 15-22, 1998.

[46] S. Nasar, "Electric Machines and Transformers," New York: Macmillan, pp.16-18, 1984.

[47] H. Beom and H. Cho, "A Sensor-based Obstacle Avoidance Controller for a Mobile Robot Using Fuzzy Logic and Neural Networks," in IEEE International Conference on Intelligent Robots and Systems, pp. 1470-1475, 1992.

[48] R. Zulfatman and M. Rahmat, "Application of Self-Tuning Fuzzy PID Controller on Industrial Hydraulic Actuator Using System Identification Approach," Malaysia, pp. 120-132, 2009.

[49] R. Arulmozhiyal, and R. Kandiban, "Design of fuzzy PID controller for Brushless DC motor," International Conference on Computer Communication and Informatics, pp. 212-230, 2012.

[50] H. Baogang, G. Mann and R. Gosine, "New methodology for analytical and optimal design of fuzzy PID controllers," IEEE Transactions on Fuzzy Systems, vol. 7, pp. 521-539, 1999.

[51] H. Li, L. Zhang, K. Cai, and G. Chen, "An improved robust fuzzy-PID controller with optimal fuzzy reasoning," IEEE Transactions on Systems, Man and Cybernetics, vol. 35, pp. 1283-1294, 2005.

[52] H. Guoshing, and L. Shuocheng, "PC-based PID speed control in DC motor," International Conference on Audio, Language and Image Processing, pp. 13-22, 2008.

[53] MPPT - Search - Search - MATLAB & Simulink (mathworks.com)